Al-Azhar Bulletin of Science, Section D, Vol. 33, No. 1 (June) 2022, pp.143-163
http://doi.10.21608/absb.2022.104424.1151

Al-Azhar Bulletin of Science: Section D

UTILIAZTION OF GEOPHYSICAL AND SEDIMENTOLOGICAL STUDIES IN THE ESTIMATION OF THE SUBGRADE SOIL IN BURAYDAH CITY, KINGDOM OF SAUDI ARABIA

Osama El Shafaey [a,] *, Ahmed M. Saad [b], Sherif M. ElKholy [c]

[a] Saden for Engineering Company, Cairo, Egypt.
[b] Geology Department, Faculty of Science, Al Azhar University, Cairo, Egypt.
[c] Civil Department, Faculty of Engineering, Al Qassim University, Al Qassim Region, Kingdom of Saudi Arabia.
* Corresponding Author: saden.egy@gmail.com.com

Received: 17 Nov 2021; Revised: 21 Dec 2021; Accepted: 01 Jan 2022; Published: 01 Jun 2022

ABSTRACT

With the continuous increase in population and economic and vital activities in Saudi Arabia and the entire world, there has become a significant increase in the construction activities. So, an appropriate investigation was carried out to assess the geotechnical parameters to verify the suitability of Buraydah area for the urban extension using shallow seismic refraction technique and sedimentological studies. For this purpose, fifteen seismic refraction spread and fifty nine sediment samples conducted in the study area. The sedimentological study includes; grain size analysis, to evaluate the textural parameters and statistical measurements to describe the depositional pattern of the studied sediments in the area. The statistical parameters include; graphic mean size varying from (-1.7ϕ) to (0.44ϕ), the sorting (σI) ranges from (1.3ϕ) to (2.2ϕ), the skewness (Sk) ranges from (-0.08ϕ) to (0.97ϕ), and the kurtosis (Kg) ranges between (0.57ϕ) to (2.2ϕ). In addition, this study was supported by microscopic analysis. The foundation material indices of shallow seismic refraction technique show that the calculated values of Poisson's ratio that founding within all layers throughout the study area is (0.24), the calculated material index values is (0.05) and the estimated concentration index values is (5.2). The ultimate bearing capacity values of the surface layer where the values are ranged between 0.09 Kg/cm^2 and 136 Kg/cm^2, the second layer ranged from 2.87 Kg/cm^{2}to 185 and the third layer values are ranged between 1.9 Kg/cm^2 and 185 Kg/cm^2.

Keywords: Textural parameters; Ultimate bearing capacity; Shallow seismic refraction; Material indices; Mesokurtic and Primary wave

1. INTRODUCTION

Buraydah city is the capital of Al Qassim region, which is located at the heart of Saudi Arabia, and almost in the center of the Arabian Peninsula. Buraydah is located in the central eastern part of Al Qassim region, on the edge of Wadi Al-Rummah. Buraydah is called the capital of dates and having an area of approximately 1300Sq.Km. It is defined by the following co-ordinates, latitude 26°14'18.16'' and 26°24' 21.20'' N and longitude 43°35'35.56'' and 44°4' 37.52'' E, and the elevation ranges from 581 to 706 m above sea level (Fig.1).

The most important problem in the study are is that there are many sandy areas ('Nafuds') surrounding Buraydah. The Buraydah Quadrangle is underlain by Phanerozoic sedimentary rocks arranged in a homocline sequence of beds. This system determines a succession of parallel cuestas, trending north-northwest and facing west and southwest, separated by depressions of varied width commonly occupied by eolian deposits (Nafud), such deposits cover a substantial area in the

eastern part of the Quadrangle (1). The cuestas are all cut diagonally from southwest to northeast by the Wadi Al-Rummah, which is now largely sanded up by Nafud Al Thuwayrat. In the Buraydah Quadrangle there are two main geomorphologic units represented by dune systems and wadi Al-Rummah. The dune systems ('Nafuds') cover about a third of the total area of the quadrangle and contain both active and inactive dunes. The main Nafuds e.g (Al Thuwayrat, Nafud as Sirr, Nafud Ashshuqayyiaqah, Nafud Al Ghamis and Nafud at Tarafiyah) are scattered through along the bed of Wadi Al-Rummah. Wadi Al-Rummah is one of the Arabian Peninsula's longest river valleys, at a length of almost 600 km (370 mi).

Refraction surveys are widely used to study the water table, engineering purposes of the poorly consolidated layers near the ground surface, and in determining near-surface corrections for deep reflection traces. The multichannel analysis of surface wave (MASW) has proven its efficiency for fracture investigation and near surface geotechnical characterization of the ground (2) and (3). The results of MASW can reveal valuable information on the shear wave velocities, Primary wave /shear wave (Vp/Vs) ratio and Poisson's ratio that are important for understanding the properties of the rocks affected by the fractures.

In this study, the main application of the seismic refraction is to delineate the subsurface layering and velocities. Geoseismic cross sections are constructed; these sections reflect the number of layers penetrated by the seismic waves. Also, the type of lithology of each layer is determined according to the values of velocities of seismic waves through layers and the geologic structures, that may affect the shallow subsurface section.

Several studies have been carried out on Buraydah city and the area of Qassim region as a whole. Many workers among them have carried out these studies are; (4);(5); (6); (7);(8); (9) and (10).

The main objective of the present paper is to study the geotechnical properties of the foundation beds to be suitable for construction using a combination of shallow seismic refraction technique and sedimentological studies.

2. GEOLOGICAL SETTING OF SITE INVESTIGATION

The stratigraphy and geology of the Buraydah Quadrangle were studied by many authors such as; (11);(12);(13) and (14). The entire Buraydah Quadrangle is underlain by Phanerozoic sedimentary rocks of the western edge of the sedimentary basin that occupies the Arabian Shelf. These sedimentary rocks are cropped out and have been assigned to the following lithologic Formations of Paleozoic and Mesozoic age. Buraydah city lies in khuff Formation that is formally defined by (10), was amended by (11), more recently, (12) revised the type section for formation in the Ad Dawadimi Quadrangle and divided it informally into Unayzah, Huqayl, Duhaysan, Midhnab and Khartam members. The Khuff Formation in the Buraydah Quadrangle, with the thickness of 264 m south of Wadi Al-Rummah and 222 m north of Wadi Al-Rummah) crops out in west-southwest-facing cuestas, such as Safra , Unayzah, Jal Khartam, Jal al Watah, in a belt of fairly constant width that interrupted by Wadi Al-Rummah. Buraydah City lies exactly in the Unayzah member of Khuff Formation. The Unayzah member lies disconformably on the pre Khuff paleosurface and begins a conformable succession that continuous to the late Triassic Minjur Sandstone. In general, the Unayzah Formation is composed of cycles of cross-bedded, fine to coarse-grained quartz sandstones, siltstone, vary-colored clay stones, and thin beds of argillaceous limestone (Fig.2).

The study area contains abundant faults with meter-scale throws. They show the following preferential strikes: (1) Northwest in the Saq sandstone, and the Qaseem, Zarqa, Sarah, Khuff, and Jilh Formations. This fault direction is accompanied by east - striking fault network. (2) Northeast visible in virtually all outcrops. (3) N. 5 E. in the southern part of the Quaderangle. These faults, such as the ArRish fault, represent the prolongation of the faults known in the Al Faydah Quadrangle and display throws of several meters in the Khuff Formation.

3. MATERIALS AND METHODS

Fifteen seismic refraction compressional (P-wave) spreads were conducted in the study area which have length (120m), number of geophone (24), geophone spacing (5m) (Fig. 3). The shallow seismic refraction survey was conducted along the proposed spreads using a seismograph model (Mcseis-170 f, OYO). It is a modern engineering refraction and simple reflection seismograph system. The used seismograph has memory length of 1024 or 2048 words/ channel. It has a digital recording capability, so the seismic signal from each geophone can be viewed instantaneously.

Seismic refraction data were processed using Winsism software (version-11), which prepared by Geosoft (2009) acquired seismic refraction data picked, plot travel time-distance curves and analyzed, as well as interpreted with applying the generalized reciprocal method (GRM Method). A total of fifty nine representative sediment samples were collected from the different localities of the study area for laboratory analysis. Each sample was sieved at half phi intervals down to a 27 μm (5 ϕ) sieve (15). Subsequently, the sediment was analyzed using Gradistat software version 8.0 (16) with the grain size classification of Wentworth (17). Petrographic analyses of the sedimentary rock samples including the detailed description of these samples by using microscopic examination of the 27 thin sections, for identification of their textural, compositional classification and diagentic characteristics for each rock type.

4. RESULTS AND DISCUSSION

4.1. Sedimentological Studies

The sedimentological studies include grain size analysis of coarse grained soil, thin section of rock samples. The different sedimentary facies forming the sedimentary succession and their mutual relationships are to be emphasized. The depositional interpretations will be given to recognize the evolution of these sediments.

4.1.1. Statistical Parameters

Grain size analysis is used for many purposes, such as textural, description, examining the behavior of sediments during transportation and deposition. It is also used to interpret the environmental of deposition of clastic sediments, and to estimate the subsurface sediments (15) and (18). The results of the mechanical analysis are tabulated in Table (1) and the data are represented by cumulative curve (Fig. 4). The statistical parameters were calculated according to the formulas of (15), and the results are shown in Table (1). It was found that, the graphic mean size values from (-1.7 Φ) to (0.44 Φ) with an average of (-0.63 Φ) falling in very coarse sand grade, the majority of the examined samples are very coarse sand (48 samples), while few of them are coarse sand (11 samples). The values of sorting coefficient (σI) range from 1.3 Φ (poorly sorted) to 2.2 Φ (very poorly sorted) with an average 1.75 Φ falling in the poorly sorted. The majority of the studied samples are poorly sorted (45 samples), while the few samples are very poorly sorted (14 samples). The skewness ranges from -0.08 Φ (near-symmetrical) to 0.97 Φ (strongly fine-skewed) with an average of (0.45 Φ) falling in the strongly fine-skewed. The kurtosis values range from 0.57 Φ (very platykurtic) to 2.2 Φ (very leptokurtic) with an average 1.39 Φ proving (leptokurtic). Coarse grained soils or granular soils (sand and gravel) which have good load bearing capacities and good drainage qualities, and their strength and volume change characteristics are not significantly affected by change in moisture conditions. So this type of soil is suitable for direct foundation above them, and that from the stand point of engineering geology.

4.1.2. Depositional Environment

Two scatter diagram plots of statistical parameters calculated from grain size distributions of sand after (19) and (20) are applied in this study to indentify the mode and different depositional environment. Friedman (19) concluded that a plot between skewness and standard deviation is most effective in differentiating river and beach sands. By applying this relationship for the investigated sediments the examined samples lie in the river field (Fig. 5). Moiola and Weiser (20) used the textural parameters derived by (15) in various combinations as environmental indications. They found that a plot diagram between (σ_I) against (Mz). This diagram shows that, the

studied samples are deposited in the river environment (Fig.6).

4.1.3. Petrographical Analysis

The thin section petrography is one of the most practical methods to express specific characteristics of the depositional environments. To accomplish these study eight thin sections were prepared representing the encountered lithologies. The petrographical analysis of Buraydah City indicated the presence of two microfacies types. These microfacies are calcareous quartz arenite sandstone type and dolomitic lime-mudstone carbonate type.

Calcareous quartz Arenite: This sandstone type is represented by samples 2-3, 7-4, 21-3, and 32-2. Petrographically, it is composed of about 96% quartz grains with terraces of microcline and mica grains. The quartz grains are fine-grained, moderately to well sorted, angular to sub angular, spherical to elongated and close packing fabric. Feldspar grains are partially altered into clay minerals. These siliciclactic grains are cemented by microcrystalline calcite cement (Fig. 7 a, b). In sample 32-2 the quartz grains are moderately to ill sorted. In addition, few carbonate lithoclastic grains can be observed which are composed of microcrystalline dolomitic and quartz grains (Fig.8 a, b).

Dolomitic Lime-mudstone: This carbonate lithofacies is recorded in samples 1-3, 22-2, 26-2, and 33-3. Petrographically it is composed of cryptocrystalline and microcrystalline calcite cements that occasionally dolomitize into euhedral (ideotopic) microcrystalline, equigranular, planner dolomite crystals. Few (less than 3%) silty quartz grains can be noted in this microfacies type. Iron oxide stains can be detected in this carbonate microfacies (Fig.9 a, b).

4.2. Geophysical Studies

4.2.1. Seismic Refraction Data Interpretation

Seismic refraction measurements are complied principally to study the characteristic of subsurface layering. The interpretation of seismic refraction data aims to define the following: (A) geoseismic cross section and that include P-wave velocity, depth and thickness of subsurface layers. (B) Parameters resulted from equations based on (21);(22);(23) and that include the following: (1) Shear wave velocity and rock density of subsurface layers and areal distribution maps of these parameters within each layers, 2) Material indices (N-value, Poisson's ratio, material index, concentration index and stress ratio.

4.2.1.1. Geoseismic Cross Section

Geoseismic cross sections or depth-velocity models are constructed along each spread, which interpreted by GRM method. Time-distance curves and then interpreted depth-velocity sections of these spreads are shown in (Figs. 10 and 11). Tables (2 and 3) shows the primary and secondary wave velocities values of common rocks and soil materials (24) and (25). Igneous and metamorphic rocks typically have high velocity values. The velocities of these rocks are greatly dependent on the degree of fracturing and the percentage of the fractures filled with groundwater. Sedimentary rocks, which usually are more porous and have higher water content, normally have lower velocity values than igneous and metamorphic rocks.

The seismic primary waves velocities distribution analysis indicated that, there are three different zones ranging between (500 – 625 m/s), (1300 – 1900 m/s) and (2200 – 3000 m/s). The obtained results show that the first geoseismic layer corresponding to unconsolidated wadi sediments while the second geoseismic layer is represented by consolidated wadi sediments and the third layer reflected that fracture sandstone layer. The estimated thickness of the first layer varies between 1 m to 8 m and the second layer ranges between 3.5 to 42 m Table 4.

4.2.1.2. Calculation of foundation material indices

Material indices that determined throughout the examination area represented by (N-value, Poisson's ratio, material index, concentration index and stress ratio). Table (5) shows the values of N-value throughout the study area based on Bowels (26). The calculated values that found throughout the first layer ranging from (32 to 55) which reflected that dense materials founding within this layer, while the values within the second and third layers are more than (50) means that very dense materials

founding within these layers (Fig.12). The calculated values of Poisson's ratio that founding within all layers throughout the study area is (0.24) and this value according to (27);(28);(29) and (22) means that the types of materials within the study area are competent materials.

The calculated material index values within all layers of the study area is (0.05) and this value according to (27);(28) and (29) reflected that competent materials founding within the study area. The estimated concentration index values that founding within all layers throughout the examination area is (5.2) and this value give an indication about the degree of material competent and this indication is moderate competent materials according to (30). The calculated values of stress ratio that founding within all layers of the study area is (0.30) and this value give an indication about degree of material competent and this indication is good competent materials according to (30).

4.2.1.3. Ultimate Bearing Capacity (Qult)

The ultimate bearing capacity (Qult) can be defined as "the maximum load required for shear failure or sand liquefaction". This capacity is controlled by shear strength factor. The ultimate bearing capacity for cohessionless soils can be calculated by using the standard penetration test (SPT) from parry's formula (31) as:

$$Qult = 30\ N \quad (1)$$

Where "N value" is the resistance to penetration by normalized cylindrical bars under standard load. The relation between shear wave velocity and N-value for sandy and clayey soil is given by (32) and (33) as:

$$Vs = 89.9\ N\ 0.341 \quad (2)$$

The relation between the ultimate bearing capacity and shear wave velocity is given by (34) as:

$$Qult = 10\ 2.932\ (\log Vs - 1.45 \quad (3)$$

The low ultimate bearing capacity values of the surface layer are observed in the southern parts of the study area that indicates to low ultimate bearing capacity material. The high values of this parameter are occupied in the northern parts of the study area, which indicate the moderate ultimate bearing capacity material. The distribution of the ultimate bearing capacity in the second layer is shown in (Fig. 13). This parameter's values ranged from 2.87 Kg/cm^2 to 185 Kg/cm^2, where the very low values of this parameter are observed in the northeastern parts of the study area, which may reflect the low ultimate bearing capacity materials. The highest values of this parameter noted in the northwestern. Figure 13 shows the calculated ultimate bearing capacity of the third layer the values are generally ranged between 1.9 Kg/cm^2 and 185Kg/cm^2. The low values are observed at the southeastern part of the study area that indicates to very low ultimate bearing capacity material. The high values of this parameter are occupied around the south and northwestern parts of this area.

5. CONCLUSIONS

This study is combining of the sedimentological and geophysical studies to evaluate the subsurface soil in Buraydah city. The gathered information will be useful in the management and development of the area under study. The statistical parameters include; graphic mean size, sorting, skewness and kurtosis, indicating the studied sediments varying from coarse to very coarse grade sand. The fluctuation between poorly sorted to very poorly sorted, and from near symmetrical to fine skewed under very platykurtic to very leptokurtic. From the relationships between the statistical parameters, the textural characteristics strongly suggest that river conditions were most probably the dominating factors controlling the transportation and accumulation of the investigated sediments. Shallow seismic refraction parameters indicate that the foundation materials are dense to very dense, moderate to good competent materials based on the results of the foundation indices. The low ultimate bearing capacity values of the second layer are observed in the northeastern parts of the study area, which may reflect the low ultimate bearing capacity materials, while the highest values noted in the northwestern parts. The low values of the third layer are observed in the southeastern part of the study area, while the high values of this parameter are occupied around the south and northwestern parts of this area.

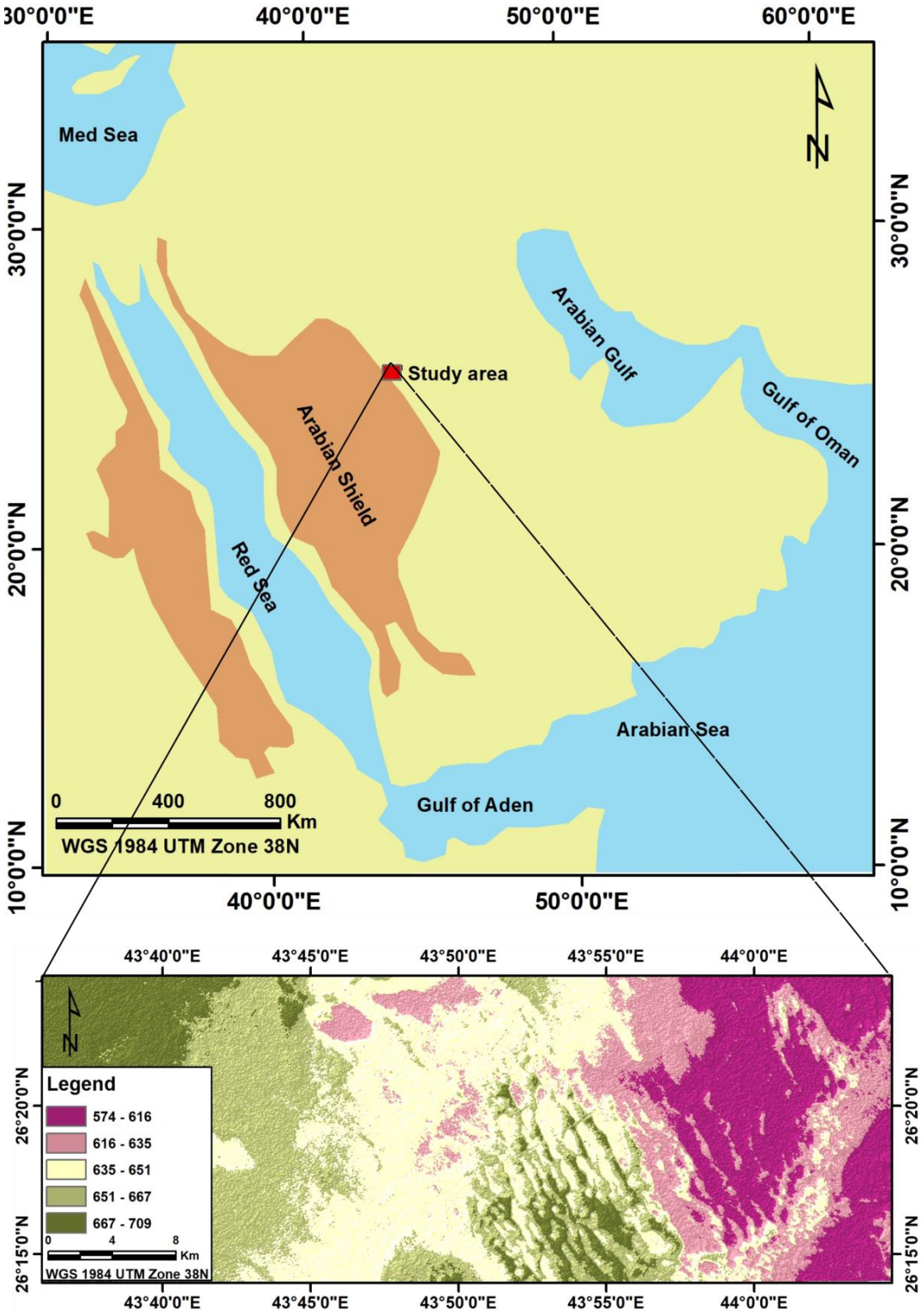

Fig. (1). Location map of Buraydah City.

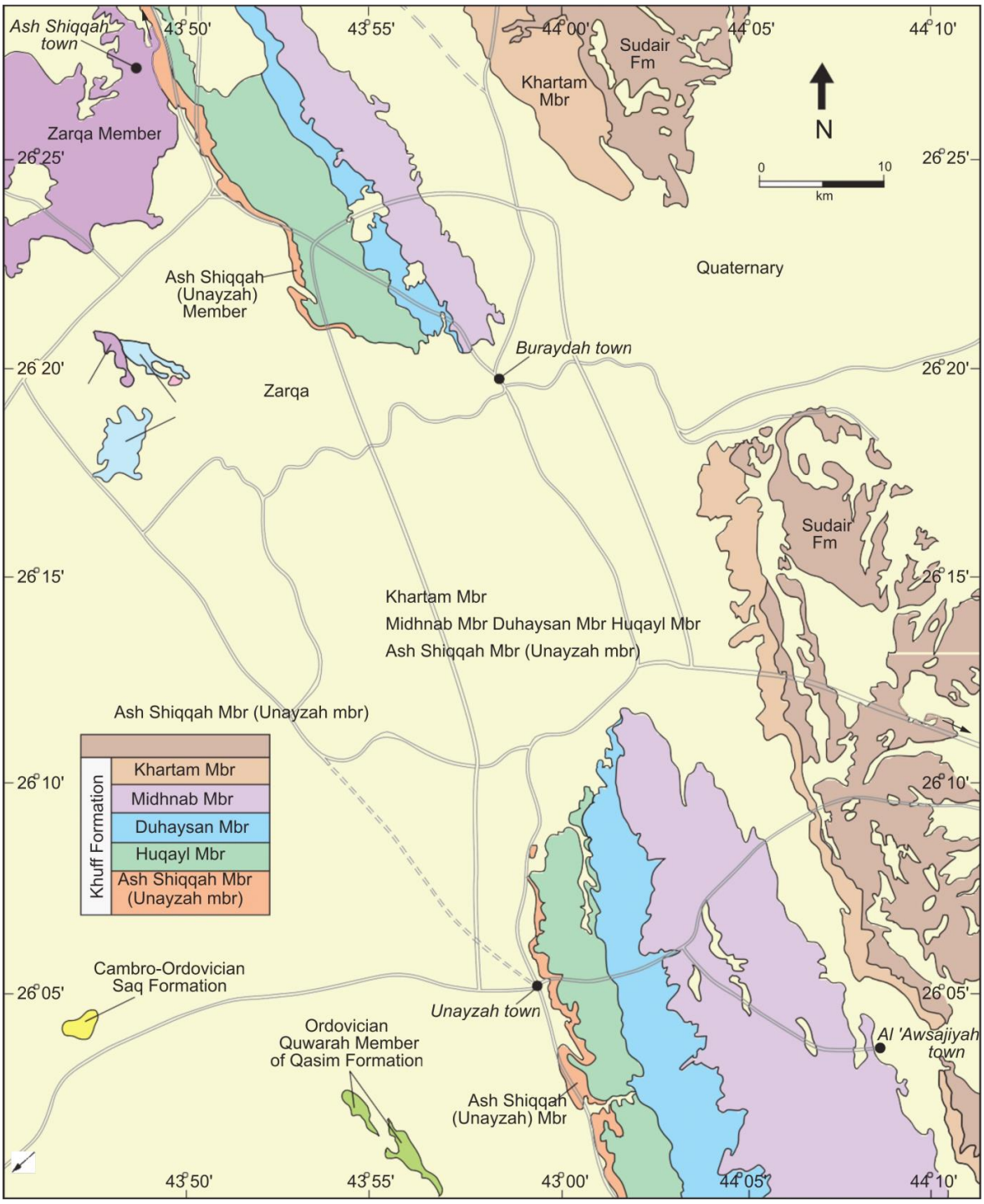

Fig. (2). Geological map of Buraydah quadrangle after (14).

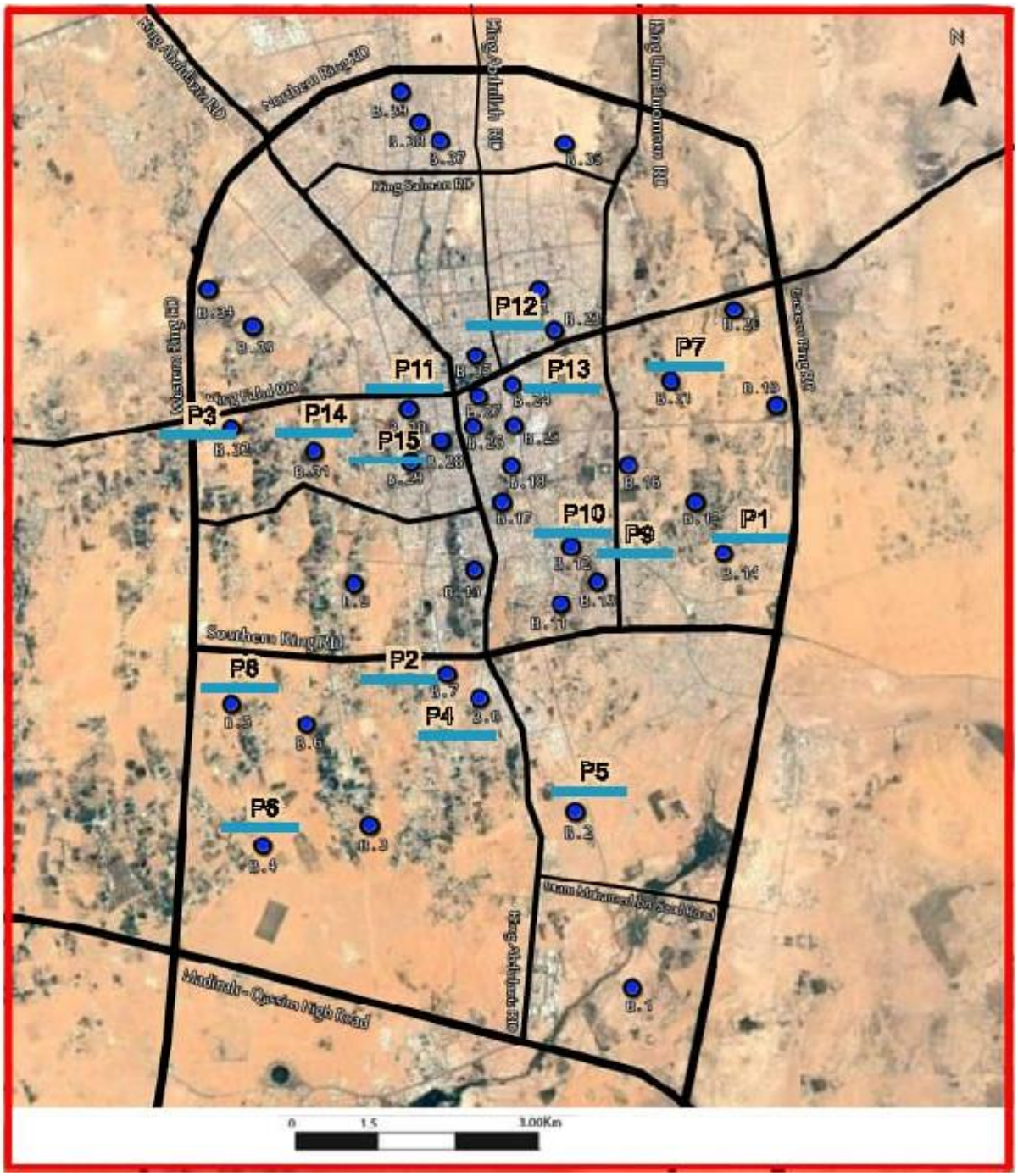

Fig. (3). Location map of seismic refraction spreads of the study area

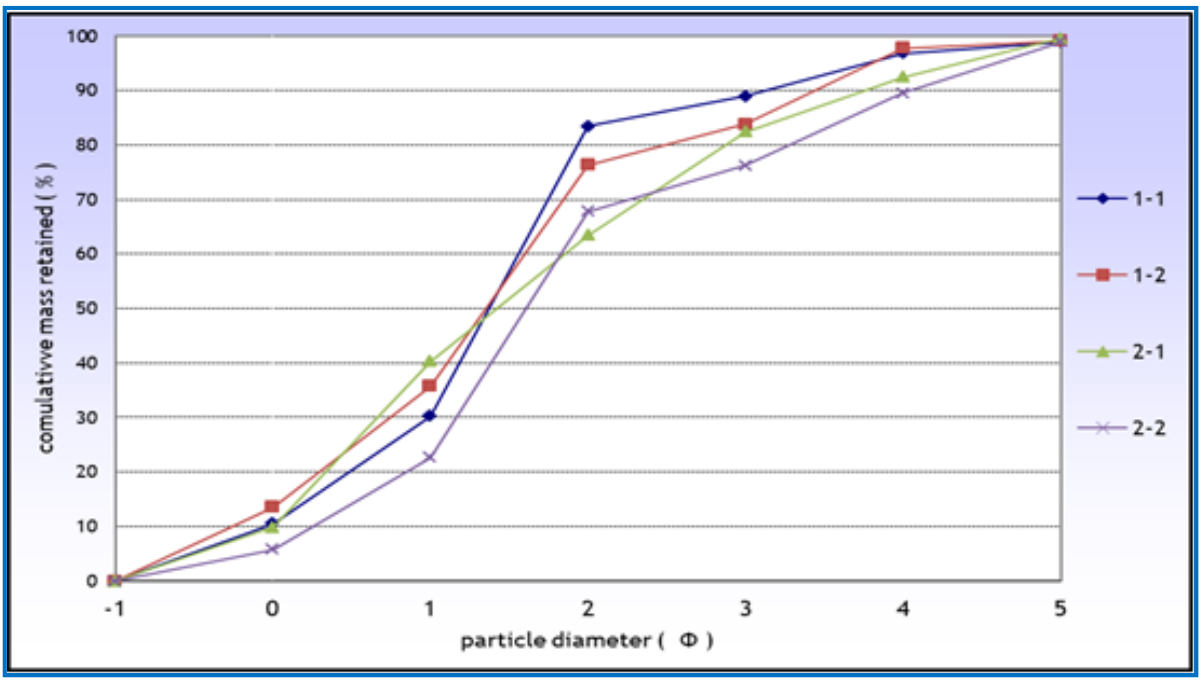

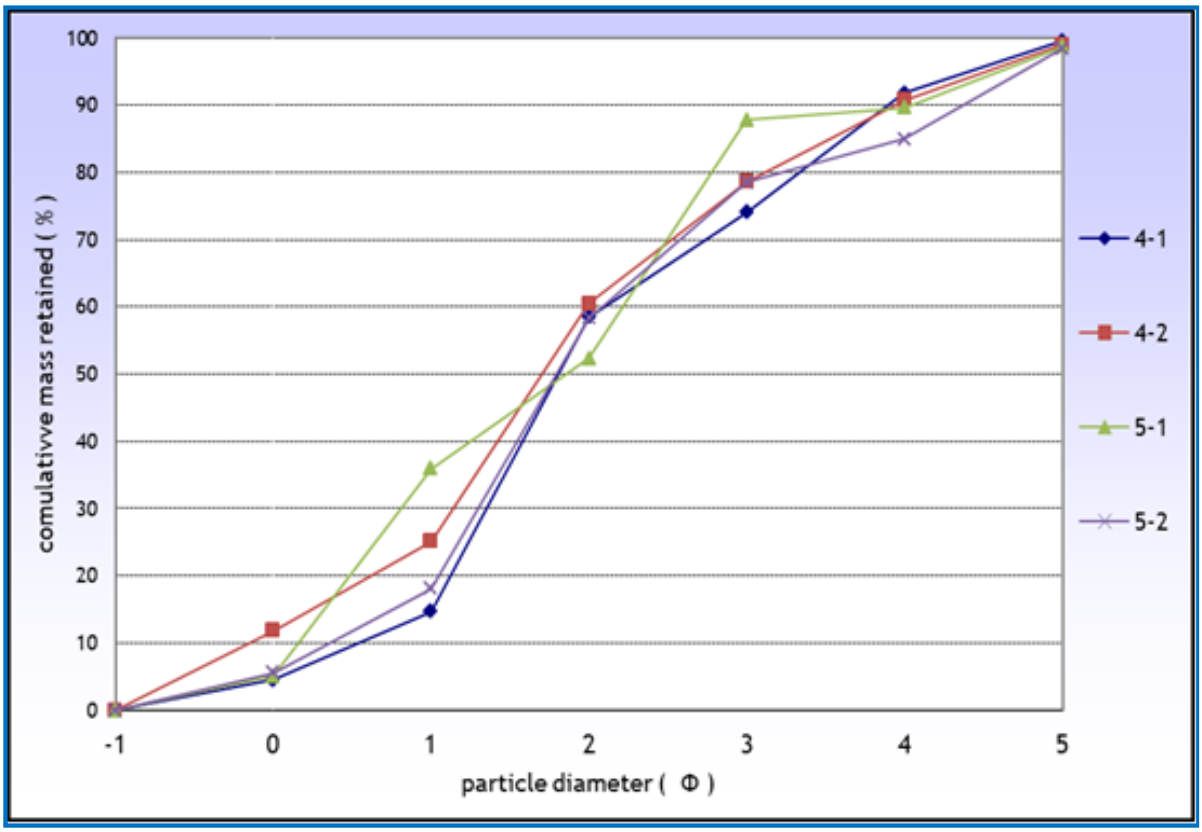

Fig. (4). Cumulative curves (phi)of the some studied samples.

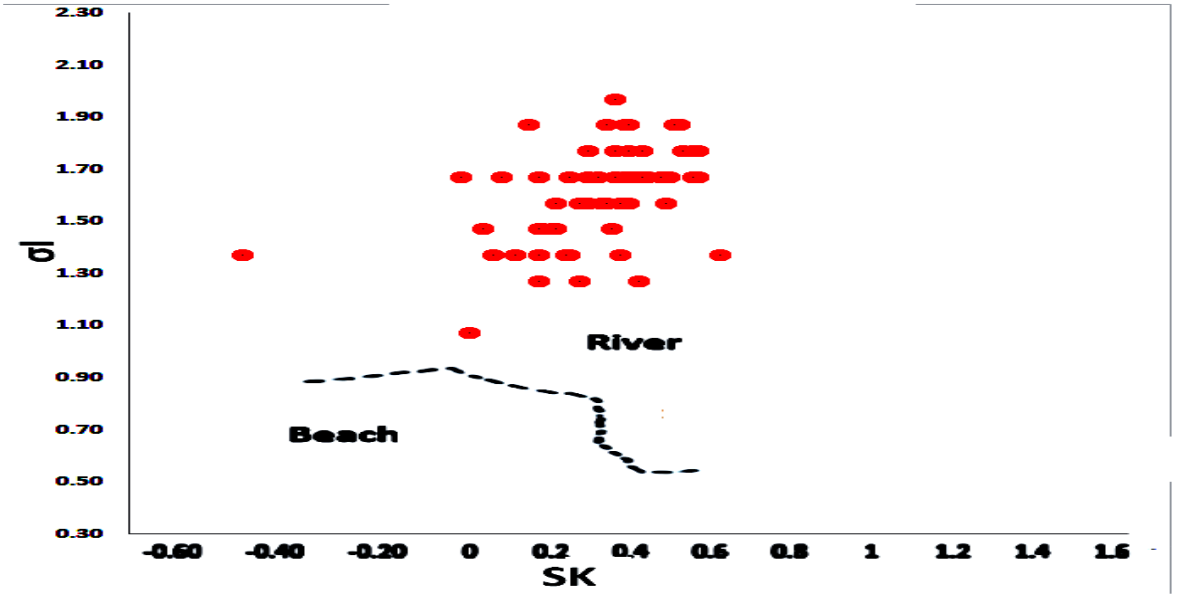

Fig. (5). Plot of inclusive graphic standard deviation (σ_I) versus inclusive graphic skeweness (SK) of the sieved samples on diagram of (19)

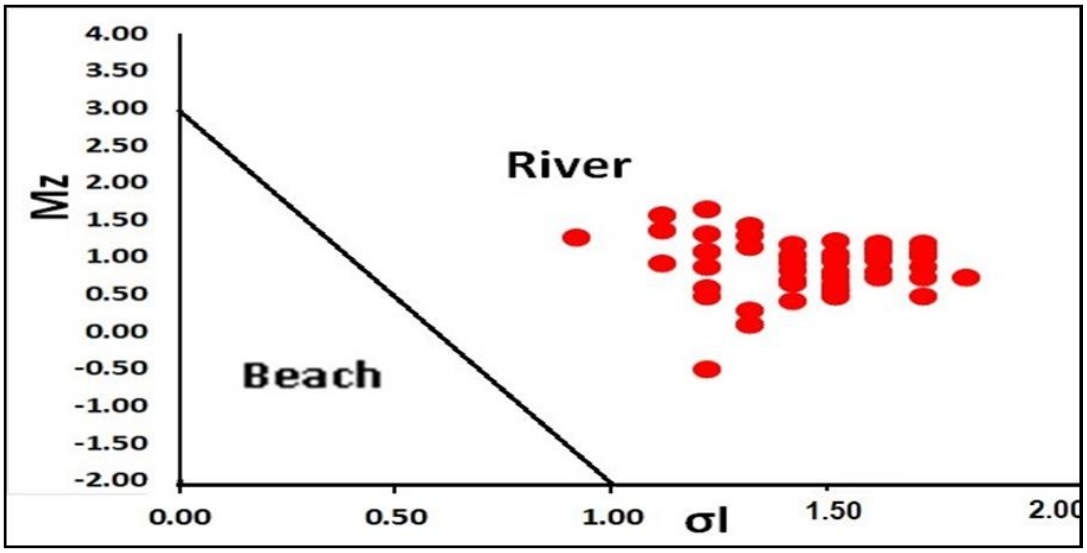

Fig. (6). Plotting of mean size (M_Z) versus standard deviation (σ_I) relation of the analyzed samples on diagram of (20)

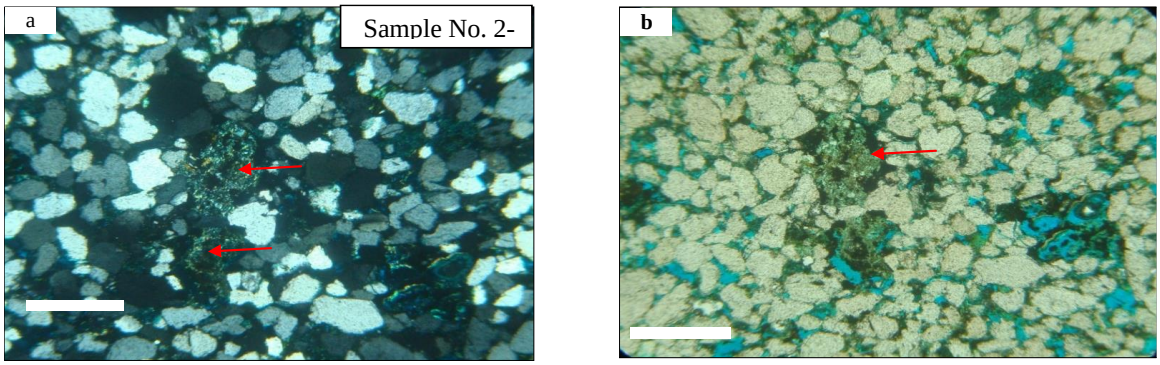

Fig. (7). Microphotographs showing quartz arenite sandstone type. Some feldspars grains are partially altered to clay matrix (arrows). a) PPL; b) ordinary light. Bare scale = 250µm

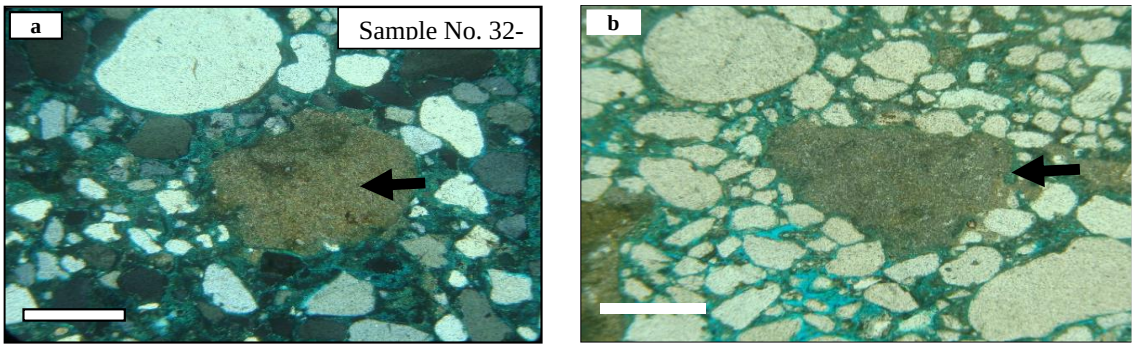

Fig. (8). Microphotograph showing quartz arenite sandstone type. Some microcrystalline dolomitic grains are observed (arrows).a) PPL; b) ordinary light. Bare scale = 250µm

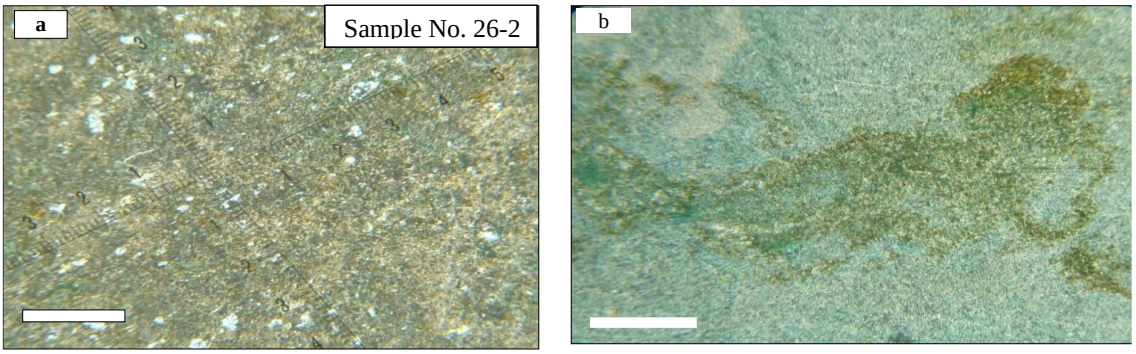

Fig. (9). Microphotograph showing dolomitic Lime-mudstone (silty quartz grains and terraces of iron oxides). a) PPL; b) ordinary light. Bare scale = 250µm

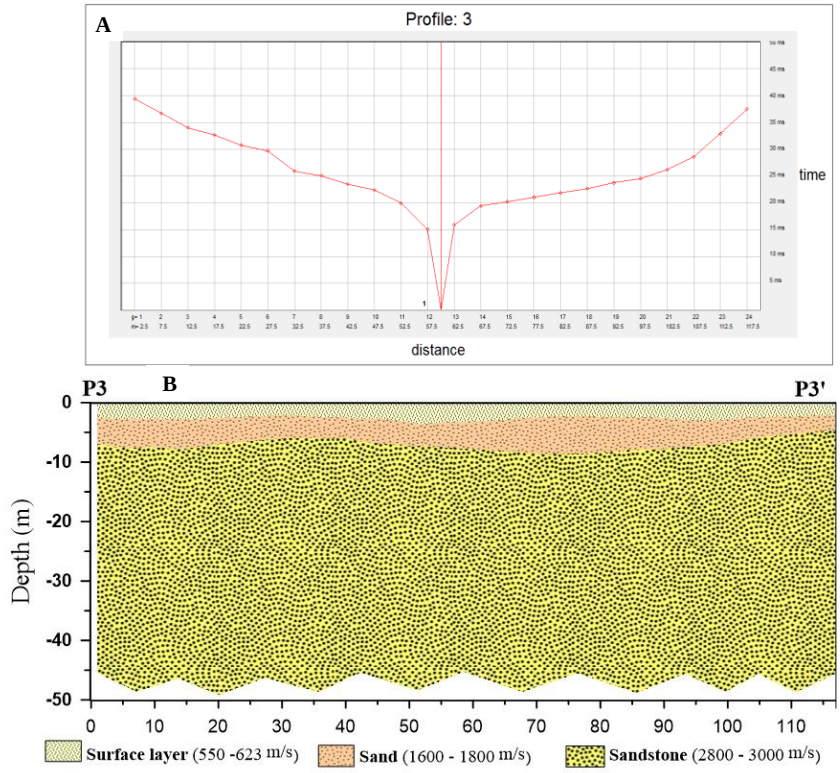

Fig. (10). T–D curve and geoseismic cross section along spread No. (3) in the spot area (A) Time-Distance curve of (P- waves) (B) Interpreted geoseismic cross section by GRM.

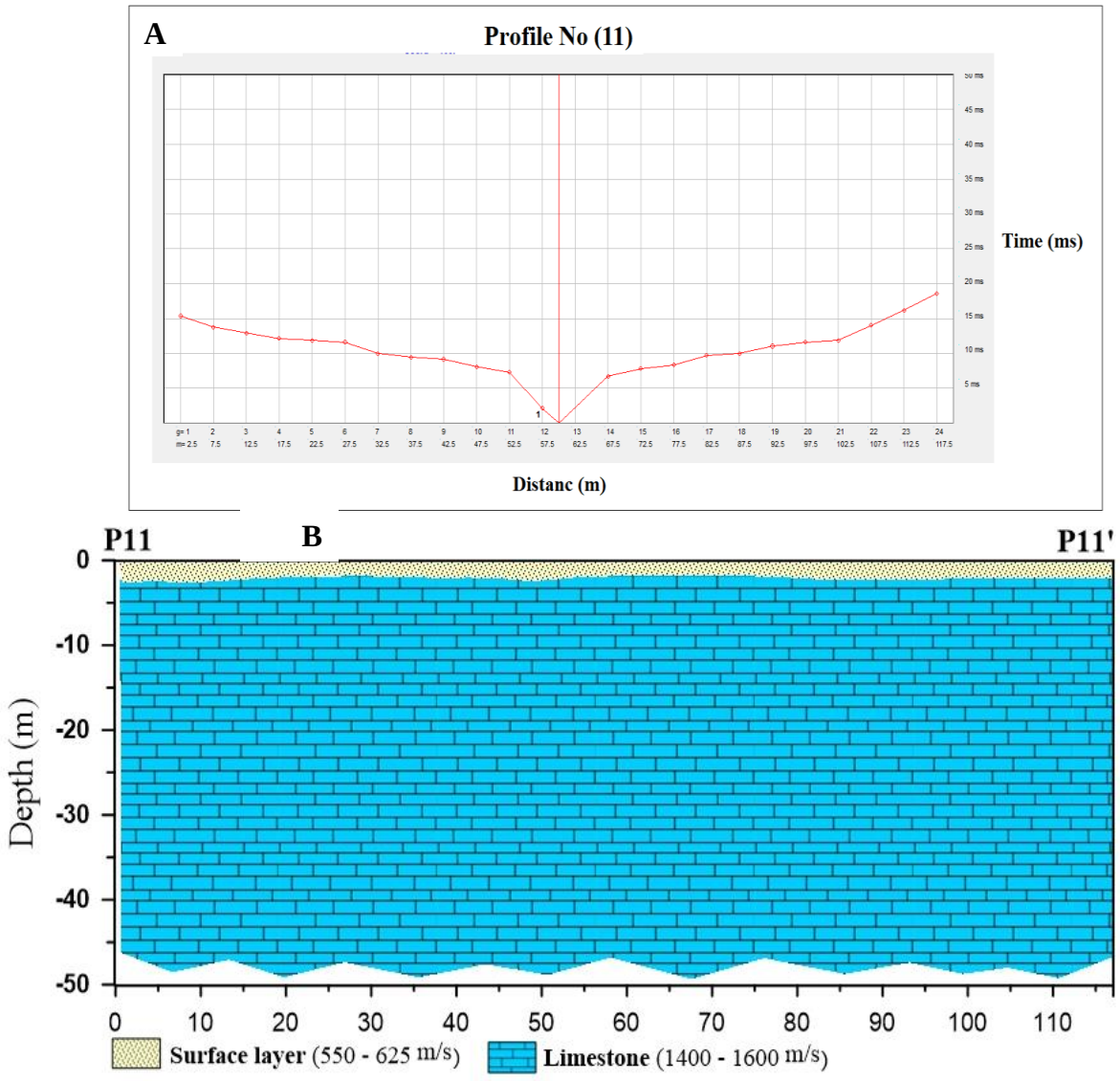

Fig. (11). T–D curve and geoseismic cross section along spread No. (11) in the spot area (A) Time-Distance curve of (P- waves) (B) Interpreted geoseismic cross section by GRM.

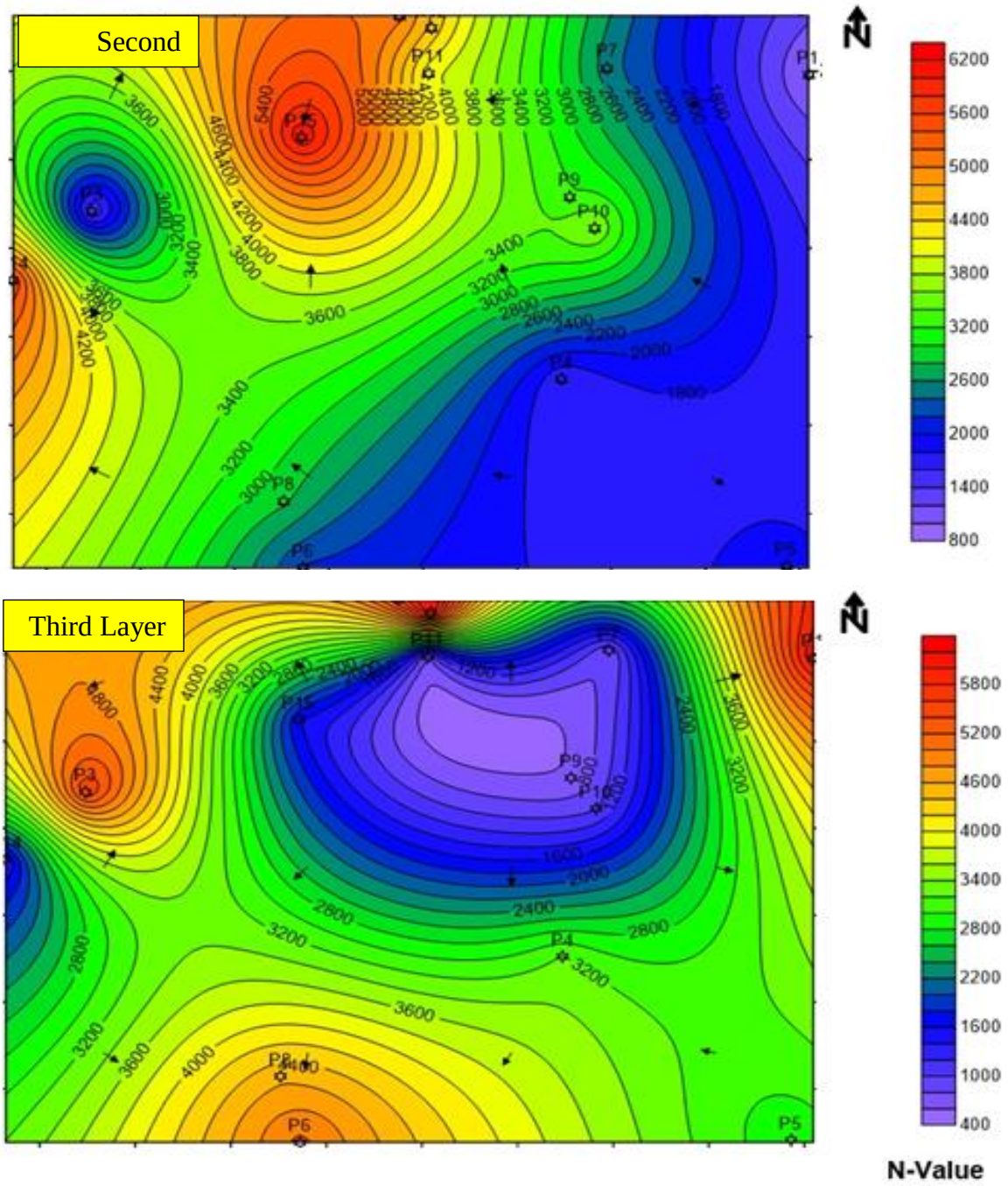

Fig. (12). A map illustrates the distribution of the N- value in the second and third layers.

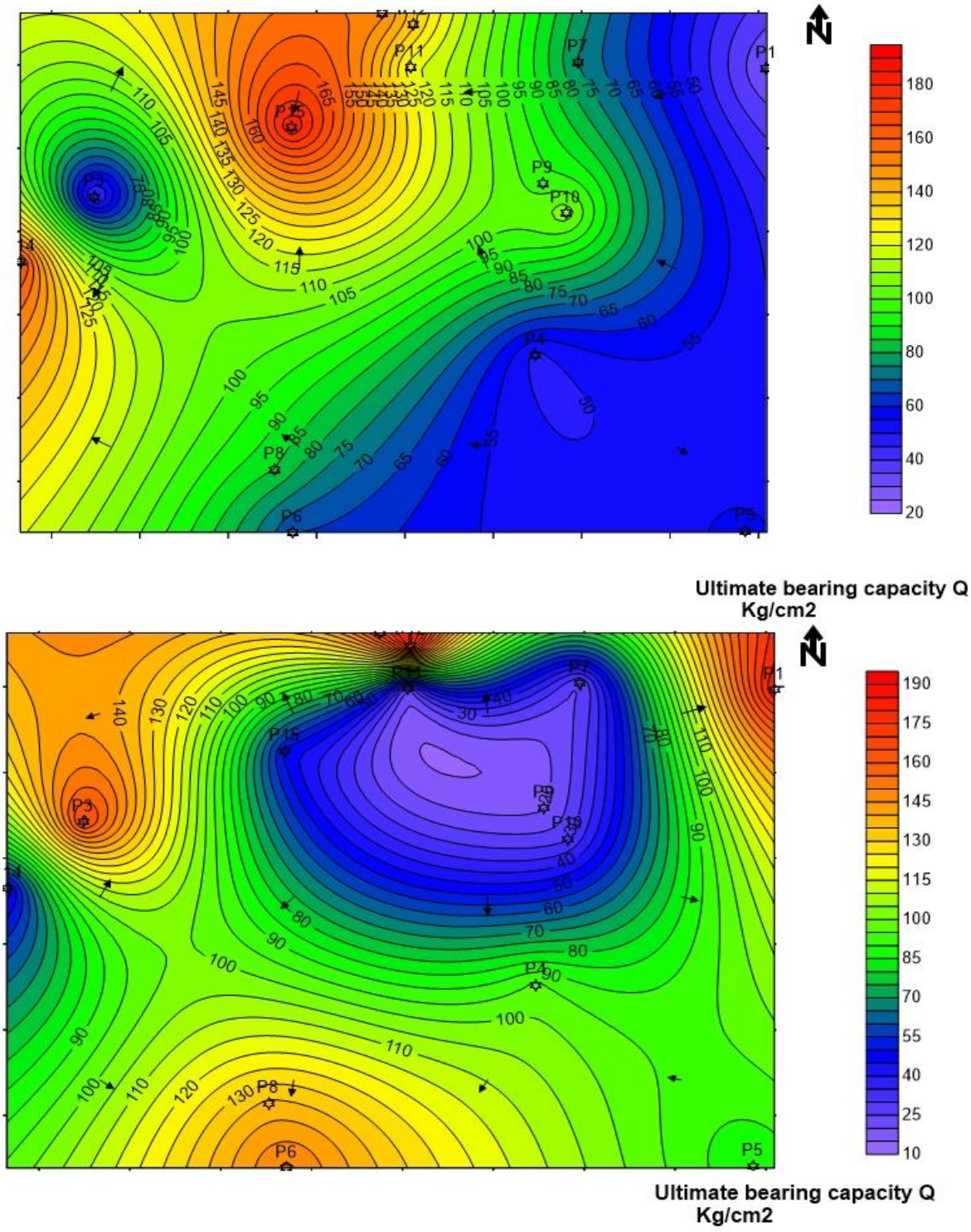

Fig. (13). A map illustrates the ultimate bearing capacity in the second and third layers.

Table 1. Statistical parameters of the grain size distribution of the studied samples

Sample No.	Texture Parameters							
	Mz	Description	σI	Description	SK	Description	KG	Description
1-1	-0.62	V.C.S.	1.6	P.So.	0.14	F.Sk.	2.2	V.L.Ku.
1-2	-0.55	V.C.S.	1.8	P.So.	0.17	F.Sk.	1.5	V.L.Ku
2-1	-0.37	V.C.S.	1.8	P So.	0.18	F.Sk.	1.2	L.Ku.
2-2	-0.06	V.C.S.	1.7	P.So.	0.29	F.Sk.	1.3	L.Ku.
4-1	0.16	C.S.	1.5	P.So.	0.32	S.F.Sk.	1.4	L.Ku.
4-2	-0.17	V.C.S.	1.8	P.So.	0.12	F.Sk.	1.5	V.L.Ku.
5-1	-0.33	V.C.S.	1.6	P.So.	-0.08	N.Sym.	1.2	L.Ku.
5-2	0.22	C.S.	1.7	P.So.	0.31	S.F.Sk.	1.6	V.L.Ku.
6-1	0.06	C.S.	1.3	P.So.	0.47	S.F.Sk.	1.7	V. L.Ku.
6-2	-0.12	V.C.S.	1.6	P.So.	0.37	S.F.Sk.	1.9	V.L.Ku.
7-1	-0.66	V.C.S.	1.9	P.So.	0.13	F.Sk.	1.1	M.Ku.
7-2	-0.50	V.C.S.	1.8	P.So.	0.21	F.Sk.	1.5	V.L.Ku.
7-3	-0.72	V.C.S.	1.6	P.So.	0.42	S.F.Sk.	0.62	V.L.Ku.
8-1	-1.7	V.C.S.	1.6	P.So.	0.97	S.F.Sk.	0.77	P.Ku.
8-2	-0.73	V.C.S.	2.1	V.P.So	0.17	F.Sk.	0.84	P.Ku.
8-3	-0.71	V.C.S.	1.9	P.So.	0.25	F.Sk.	0.63	V.P.Ku.
9-1	-0.65	V.C.S.	1.9	P.So.	0.15	F.Sk.	1.1	M.Ku.
9-2	-0.91	V.C.S.	1.7	P.So.	0.44	S.F.Sk.	0.57	V.P.Ku.
10-1	-0.16	V.C.S.	2.1	V.P.So.	0.01	N.Sym.	1.1	M.Ku.
11-1	-0.02	V.C.S.	2.1	V.P.So.	0.13	F.Sk.	0.87	P.Ku.
11-2	-0.47	V.C.S.	2.1	V.P.So.	0.34	S.F.Sk.	1.0	M.Ku.
12-1	-0.62	V.C.S.	1.9	P.So.	0.40	S.F.Sk.	0.65	V.P.Ku.
12-2	-0.79	V.C.S.	1.8	P.So.	0.28	F.Sk.	0.63	V.P.Ku.
13-1	-0.40	V.C.S.	1.9	P.So.	0.11	F.Sk.	1.2	L.Ku.
13-2	-1.1	V.C.S.	1.7	P.So.	0.32	S.F.Sk.	0.81	P.Ku.
14-1	0.44	C.S.	1.6	P.So.	0.32	S.F.Sk.	1.3	L.Ku.
14-2	0.36	C.S.	1.5	P.So.	0.10	F.Sk.	1.5	V.L.Ku.
15-1	-0.02	V.C.S.	2.0	V.P.So.	-0.03	N.Sym.	1.1	M.Ku.
15-3	-0.47	V.C.S.	2.0	V.P.So.	0.21	F.Sk.	0.83	P.Ku.
16-1	0.01	C.S.	1.9	P.So.	0.03	N.Sym.	1.2	L.Ku.
17-1	-0.23	V.C.S.	2.0	V.P.So.	0.12	F.Sk.	1.1	M.Ku.
17-2	-0.09	V.C.S.	2.0	V.P.So.	0. 02	N.Sym.	1.1	M.Ku.
18-1	-0.12	V.C.S.	1.6	P.So.	0.26	F.Sk.	1.4	L.Ku.
18-2	-0.22	V.C.S.	1.8	P.So.	0.23	F.Sk.	1.2	L.Ku.
18-3	-0.48	V.C.S.	2.2	V.P.So.	0.15	F.Sk.	0.76	P.Ku.
19-1	-0.28	V.C.S.	1.5	P.So.	0.23	F.Sk.	2.0	V.L.Ku.
19-2	-0.28	V.C.S.	1.8	P.So.	0.04	N.Sym.	1.4	L.Ku.
20-1	-0.03	V.C.S.	1.8	P.So.	0.14	F.Sk.	1.1	M.Ku.
20-2	0.11	V.C.S.	1.6	P.So.	0.25	F.Sk.	1.1	M.Ku.
21-1	-0.22	V.C.S.	1.9	P.So.	0.08	N.Sym.	1.2	L.Ku.
21-2	-0.13	V.C.S.	2.0	V.P.So.	-0.02	N.Sym.	1.2	L.Ku.
24-1	-0.25	V.C.S.	1.9	P.So.	0.05	N.Sym.	1.1	M.Ku.
25-1	-0.72	V.C.S.	1.9	P.So.	-0.02	N.Sym.	1.1	L.Ku.
28-1	-1.1	V.C.S.	1.7	P.So.	0.28	F.Sk.	0.83	P.Ku.
28-2	0.09	C.S.	1.7	P.So.	0.16	F.Sk.	1.1	M.Ku.
30-1	-0.44	V.C.S.	1.9	P.So.	0.15	F.Sk.	0.94	M.Ku.
30-2	-0.18	V.C.S.	1.9	P.So.	-0.03	N.Sym.	1.1	M.Ku.
31-1	-0.61	V.C.S.	1.9	P.So.	0.19	F.Sk.	0.98	M.Ku.
31-2	-0.40	V.C.S.	2.0	V.P.So.	0.09	N.Sym.	0.92	M.Ku.
32-1	-0.19	V.C.S.	2.1	V.P.So.	0.12	F.Sk.	0.83	P.Ku.
32-2	-0.72	V.C.S.	1.9	P.So.	0.32	S.F.Sk.	0.65	V.P.Ku.
33-1	-0.47	V.C.S.	1.9	P.So.	0.09	N.Sym.	0.97	M.Ku.
33-2	-0.15	V.C.S.	1.9	P.So.	0.09	N.Sym.	1.1	M.Ku.
34-1	-0.19	V.C.S.	1.9	P.So.	0.08	N.Sym.	1.1	M.Ku.
34-2	-0.15	V.C.S.	2.0	V.P.So.	0.15	F.Sk.	1.2	L.Ku.
35-1	-0.57	V.C.S.	1.9	P.So.	0.21	F.Sk.	0.74	P.Ku.
37-1	-0.65	V.C.S.	1.9	P.So.	0.49	S.F.Sk.	0.60	V.P.Ku.
37-2	-0.33	V.C.S.	2.1	V.P.So.	0.02	N.Sym.	1.1	M.Ku.
38-1	-0.09	V.C.S.	2.1	V.P.So.	0.01	N.Sym.	0.91	M.Ku.

V.C.S.	Very coarse sand	N.Sym.	Near Symmetrical	L.Ku.	Leptokurtic
C.S.	Coares Sand	F.Sk.	Fine Skewed	P.Ku.	Platykurtic
P.So.	Poorly Sorted	S.F.Sk.	Strongly Fine Skewed	M.Ku.	Mesokurtic
V.P.So.	Very Poorly Sorted	M.Ku.	Mesokurtic	V.L.Ku.	Very Leptokurtic
				V.P.Ku.	Very Platykurtic

Table 2. P-waves velocities of common rock types, (after 25 and 26).

Material	P-wave Velocity (m/s)
Weathered layer	300 – 900
Soil	250 – 600
Clay	1100 – 2500
Unsaturated sand	200 – 1000
Saturated sand	800 – 2200
Unsaturated sand and gravel	400 – 500
Saturated sand and gravel	500 – 1500
Sandstone	1400 – 4300
Limestone	5900 – 6100
Anhydrite	4100
Shale	2100 – 3400
Water	1400 – 1600
Air	331.5
Granite	5000 – 6000
Granodiorite	4780
Diorite	5780
Gabbro	6450
Basalt	5400 – 6400

Table 3. Seismic velocities of earth materials.

Material	P-wave Velocity (m/s)	S-wave Velocity (m/s)
Air	332	
Water	1400 - 1500	
Petroleum	1300 - 1400	
Steel	6100	3500
Concrete	3600	2000
Granite	5500 - 5900	2800 - 3000
Basalt	6400	3200
Sandstone	1400 - 4300	700 - 2800
Limestone	5900 - 6100	2800 - 3000
Sand(Unsaturated)	200 - 1000	80 - 400
Sand (Saturated)	800 - 2200	320 - 880
Clay	1000 - 2500	400 - 1000

Table 4. Average values of primary wave velocities, thicknesses, shear wave velocities and rock densities of subsurface layers throughout the study area.

Spread No.	Primary wave velocities (m/s)			Thicknesses (m)		Shear wave velocities (m/s)			Rock densities (g/cc)		
	Vp_1	Vp_2	Vp_3	T_1	T2	Vs_1	Vs_2	Vs_3	ρ_1	ρ_2	ρ_3
1	525	1600	3000	1.0	9.0	308.824	941.176	1764.706	1.75	1.83	2.42
2	500	1700	2200	1.5	25.0	294.118	1000	1294.118	1.71	1.92	2.51
3	623	1800	2900	1.0	6.0	366.471	1058.82	1705.882	1.73	1.85	2.62
4	550	1900	2400	1.5	27.0	323.529	1117.65	1411.765	1.69	1.79	2.35
5	600	2000	2300	1.0	6.0	352.941	1176.47	1352.941	1.72	1.89	2.55
6	570	2100	2800	1.25	15.0	335.294	1235.29	1647.059	1.79	1.92	2.68
7	560	2200	1500	3.0	36.0	329.412	1294.12	882.3529	1.77	1.85	2.66
8	250	2300	----	8.0	35.0	147.059	1352.94	1588.235	1.82	2.44	2.66
9	500	2400	1400	1.0	11.0	294.118	1411.76	823.5294	1.74	1.84	2.42
10	600	2500	1600	1.0	11.0	352.941	1470.59	941.1765	1.68	1.79	2.39
11	570	2600	-----	3.0	42.0	335.294	1529.41	882.3529	1.82	2.48	2.64
12	2500	2700	3000	2.0	8.0	1470.59	1588.24	1764.706	1.7	1.92	2.64
13	2700	2800	2900	1.0	5.0	1588.24	1647.06	1705.882	1.72	1.89	2.58
14	530	2900	1800	1.0	13.0	311.765	1705.88	1058.824	1.68	1.78	2.52
15	550	3000	1900	1.5	3.5	323.529	1764.71	1117.647	1.71	1.83	2.68

Table 5. N-Value of subsurface layers throughout the study area

Spread No	N-value		
	N1	N2	N3
1	37.29949089	979.360159	6187.748782
2	32.32691022	1169.912542	2491.851703
3	61.61348273	1383.406557	5602.165919
4	42.75140288	1621.098293	3216.170668
5	55.17816642	1884.239133	2838.804932
6	47.47233504	2174.076022	5054.33453
7	45.07114327	2491.851703	810.4883232
8	4.234267451	2838.804932	4543.039198
9	32.32691022	3216.170668	662.0306128
10	55.17816642	3625.180254	979.360159
11	47.47233504	4067.061573	810.4883232
12	36.25180254	4543.039198	6187.748782
13	45. 3039198	5054.33453	5602.165919
14	38.35084574	5602.165919	1383.406557
15	42.75140288	6187.748782	1621.098293

REFERENCES

[1] Atif Elzein E. Geological and geotechnichal characterization of Paleozoic rocks and Cenozoic soil deposits around Buraydah Twon, Qasseem Region, KSA. UOFK;

[2] Pipan M, Forte E, Dal Moro G, Gabrielli P. Integrated seismic and GPR characterization of fractured rocks. In: Workshop on Hydrogeophysics – A Tool for Sustainable Use of Groundwater 2005, Palermo, Italy (2005)

[3] Tokeshi K, Harutoonian P, Leo CJ, Liyanapathirana S. Use of surface waves for geotechnical engineering applications in Western Sydney. Adv Geosci (2013); 35: 37–44 doi:10.5194/adgeo-35-37-2013

[4] Khalifa MA. Lithostratigraphic classification and depositional history of the Permian rocks in Al Qasim Province, Saudi Arabia. J African Earth Sci (and Middle East). 1993;16(3):329–40.

[5] Albusoda BS, Salem LA, Salem K. Stabilization of dune sand by using cement kiln dust (CKD). J Earth Sci Geotech Eng. 2012;2(1):131–43.

[6] Al Fouzan F, Dafalla MA. Study of cracks and fissures phenomenon in Central Saudi Arabia by applying geotechnical and geophysical techniques. Arab J Geosci. 2014;7(3):1157–64.

[7] Le Hérissé A, Molyneux SG, Miller MA. Late Ordovician to early Silurian acritarchs from the Qusaiba-1 shallow core hole, central Saudi Arabia. Rev Palaeobot Palynol. 2015;212:22–59.

[8] Benaafi M, Abdullatif O. Sedimentological, mineralogical, and geochemical characterization of sand dunes in Saudi Arabia. Arab J Geosci. 2015;8(12):11073–92.

[9] Alhumimidi MS, Harbi HM, Alfarhan MS, Abdelrahman K, Aiken CL V. Imaging fracture distributions of the Al-Khuff Formation outcrops using GPR and ERT geophysical techniques, Al-Qassim area, Saudi Arabia. Arab J Geosci. 2017;10(14):1–11.

[10.]Steineke M, Bramkamp RA, Sander NJ. Stratigraphic relations of Arabian Jurassic oil: Middle East. 1958;

[11] Powers RW, Ramirez LF, Redmond CD, Elberg EL. Geology of the Arabian Peninsula:. United States Department of the Interior, Geological Survey; 1966.

[12]Laboun AA. Regional tectonic and megadepositional cycles of the Paleozoic of northwestern and central Saudi Arabia. Arab J Geosci. 2013;6(4):971–84.

[13] Williams PL, Vaslet D, Johnson PR, Berthiaux A, Le Strat P, Fourniguet J. Geologic map of the Jabal Habashi quadrangle, sheet 26F. Kingdom Saudi Arab Saudi Arab Deputy Minist Miner Resour Geosci Map GM-98A (with text). 1986;

[14] Delfour J, Dhellemmes R, Elsass P, Vaslet D, Brosse JM, Le Nindre YM, Dottin O. Explanatory notes to the geologic map of the Ad Dawadimi Quadrangle, Kingdom of Saudi Arabia. Geoscience Map GM-60C, scale 1:250,000, sheet 24G. Deputy Ministry for Mineral Resources, Ministry of Petroleum and Mineral Resources, Kingdom of Saudi Arabia. 1982; 36 p.

[15] Folk RL, Ward WC. Brazos River bar [Texas]; a study in the significance of grain size parameters. J Sediment Res. 1957;27(1):3–26.

[16] Blott SJ, Pye K. GRADISTAT: a grain size distribution and statistics package for the analysis of unconsolidated sediments. Earth Surf. Proc. Landf. (2001) 26: 1237-1248.

[17] Wentworth CK. A scale of grade and class terms for clastic sediments. J Geol. (1922) 30 (5): 377-392.

[18] Boggs Jr S, Boggs S. Petrology of sedimentary rocks. Cambridge university press; 2009.

[19]Friedman GM. Dynamic processes and statistical parameters compared for size frequency distribution of beach and river sands. J Sediment Res. 1967;37(2):327–54.

[20] Moiola RJ, Weiser D. Textural parameters; an evaluation. J Sediment Res. 1968;38(1):45–53.

[21] Grant FS, West GF. Interpretation theory in applied geophysics. New York: McGraw-Hill; 1965.

[22] Sheriff RE, Geldart LP. Exploration seismology. Cambridge university press; 1995.

[23] Gardner LW. An areal plan of mapping subsurface structure by refraction shooting. Geophysics. 1939;4(4):247–59.

[24] Press F. Determination of crustal structure from phase velocity of Rayleigh waves part I: southern California. Geol Soc Am Bull.

1956;67(12):1647–58.

[25] Dobrin MB, Savit CH. Introduction to Geophysical Prospecting Mc Graw-Hill Book Co. New York (867 pp). 1988;

[26] Bowles JE. Foundation analysis and design. 1988.

[27] Birch F. Compressibility; elastic constants. Handb Phys constants. 1966;97–173.

[28] Gassman F. Seismische Prospektion. Birkhaeuser Verlag, Stuttgart, p. 417; 1973

[29] Tatham RH. V p/V s and lithology. Geophysics. 1982;47(3):336–44.

[30] Abd El-Rahman M. The potential of absorption coefficient and seismic quality factor in delineating less sound foundation materials in Jabal Shib Az Sahara area, Northwest of Sanaa, Yemen Arab Republic. Egypt, MERC Earth Sci. 1991;5:181–7.

[31] Parry RHG. Estimating bearing capacity in sand from SPT values. J Geotech Eng Div. 1977;103(9):1014–9.

[32] Imai T, Fumoto H, Yokota K. The relation of mechanical properties of soil to P-and S-wave velocities in Japan. In: Proceedings of 4th Japan Earthquake Engineering Symposium, Tokyo, Japan. 1975. p. 89–96.

[33] Stümpel H, Kähler S, Meissner R, Milkereit B. The use of seismic shear waves and compressional waves for lithological problems of shallow sediments. Geophys Prospect. 1984;32(4):662–75.

[34] Hanna A, El-Rahman MA. Ultimate bearing capacity of triangular shell strip footings on sand. J Geotech Eng. 1990;116(12):1851–63.

استخدام الدراسات الرسوبية والجيوفيزيقية في تقييم التربة تحت السطحية لمدينة بريدة, المملكة العربية السعودية

اسامه الشافعى [1] ' احمد م. سعد [2] ' شريف م. الخولى [3]

1. جيولـوجى بشـركة سـادن للهندسـة - القـاهرة – جمهوريـة مصـر العربية
2. قسـم الجيولوجيـا - كليـة العلـوم (بنـين) – جامعـة الازهـر - جمهورية مصر العربية
3. قسم ميكانيكا التربة والاساسات – كلية الهندسـة – جامعـة القصـيم – المملكة العربية السعودية

الملخص

مع الزيادة المستمرة في عدد السكان والأنشطة الاقتصادية والحيوية في المملكة العربية السعودية والعالم أجمع, أصبحت هناك زيادة كبيرة في أنشطة البناء. لذلك تم إجراء الفحص المناسب لتقييم المعاملات الجيوتقنية للتحقق من ملائمة منطقة بريدة للتوسع العمراني باستخدام تقنية الانكسار الزلزالي الضحل والدراسات الرسوبية. لهذا الغرض, تم إجراء خمسة عشر قطاع انكسارا زلزاليا وتجميع تسعة وخمسين عينة من الرواسب في منطقة الدراسة. تشتمل الدراسة الرسوبية علي التحليل الحجمي للحبيبات لتقييم المعاملات التركيبية والقياسات الإحصائية لوصف النمط الترسيبي للرواسب في منطقة الدراسة. وقد دلت المعاملات الإحصائية علي أن متوسط حجم الحبيبات يتراوح من (ϕ-1.7) إلى (ϕ0.44)، ومعامل الفرز (σI) من (ϕ1.3) إلي (ϕ2.2), ومعامل الانحراف (Sk) من (ϕ-0.08) إلي (ϕ0.97), ودرجة التفرطح (Kg) من (ϕ0.57) إلي (ϕ2.2). بالإضافة إلى ذلك ، تم دعم هذه الدراسة بالتحليل المجهري. توضح مؤشرات مادة الأساس باستخدام تقنية الانكسار الزلزالي الضحلة أن القيم المحسوبة لنسبة بواسون داخل جميع الطبقات في منطقة الدراسة هي (0.24)، وقيم مؤشر المواد (0.05), وقيم مؤشر التركيز (5.2) . وقد دلت النتائج أيضا علي أن قيم قدرة التحمل القصوى للطبقة السطحية تتراوح من($0.09\ Kg/cm^2$) إلي ($136\ Kg/cm^2$)، أما الطبقة الثانية فتتراوح من ($2.87\ Kg/cm^2$) إلى (185 Kg/cm^2) وتراوحت قيم الطبقة الثالثة بين (1.9 Kg/cm^2) إلي ($185\ Kg/cm^2$).